Journal of
Materials Chemistry B

PAPER

View Article Online
View Journal | View Issue

Cite this: J. Mater. Chem. B, 2015, 3, 7577

Electrochemical deposition to construct a nature inspired multilayer chitosan/layered double hydroxides hybrid gel for stimuli responsive release of protein†

Pengkun Zhao, Youyu Liu, Ling Xiao, Hongbing Deng, Yumin Du and Xiaowen Shi*

Received 2nd June 2015,
Accepted 19th August 2015

DOI: 10.1039/c5tb01056j

www.rsc.org/MaterialsB

In this study, we report a single electrodeposition process to fabricate multilayered chitosan/layered double hydroxides (LDHs) hybrid hydrogels for stimuli responsive protein release. LDHs nanoplatelets with a regular hexagonal shape were synthesized by a hydrothermal method, and a model protein, insulin, was adsorbed on the surface of the LDHs (INS-LDHs) *via* electrostatic interactions. The insulin loading ratio could reach 20% (w/w); the INS-LDHs were characterized by energy dispersive spectrometry (EDS), Fourier transform infrared spectroscopy (FT-IR), thermogravimetric analysis (TG) and zeta potential measurements. Co-electrodeposition of chitosan and INS-LDHs generated an inorganic and organic composite hydrogel with a multilayered structure, as revealed by scanning electron microscopy (SEM). The hybrid hydrogel dramatically reduced the burst release of insulin from INS-LDHs. Notably, the release of insulin was sensitive to the presence of anions, pH, and external potentials. These results suggest that co-electrodeposition of a stimuli-responsive polymer and nanoplatelets is an alternative and facile method to construct hierarchically structured hybrid hydrogels and demonstrate the great potential of the multilayered structure in drug delivery.

1. Introduction

Nature has created many intriguing structures that demonstrate exceptional biological or mechanical properties and functionalities. Thus, people devote enormous efforts to mimic structures from nature and have produced many materials having similar or even better performance than natural products.[1–3] The brick-and-mortar construction in nacre and bone is a highly oriented layered structure made from organic and platelet inorganic components.[4,5] There are numerous studies on mimicking this layered hybrid structure.[4,6] However, most of the contributions focus on improving the mechanical properties. Thus, the discovery of new applications in diverse fields is meaningful for better understanding of this nature inspired structure.

A commonly used bottom-up method to build multilayered hybrid structures is the layer-by-layer (LBL) approach, which is efficient but time consuming.[7] A recent report on electrophoretic deposition (EPD) demonstrates that nanoplatelets can be oriented into an aligned structure under an electric field.[8] EPD is a rapid and scalable process that can simultaneously assemble positively charged nanoplatelets and cationic polyelectrolytes.[9] To the best of our knowledge, the co-deposition of stimuli-responsive natural polymers and nanoplatelets to fabricate a multilayered structure has never been reported. In addition, the stimuli drug release behavior from the brick-and-mortar structure is not well investigated. Thus, in this study, we construct a layered structure by the electrodeposition method and investigate the drug release behavior in response to external stimuli.

Chitosan is a unique cationic polysaccharide containing amino groups and having important applications in drug delivery, biomedicine and tissue engineering.[10,11] It shows a pH responsive sol–gel transition and can be deposited as a hydrogel on an electrode when biasing a negative potential. The *in situ* sol–gel transition is induced by an increased pH gradient due to the consumption of protons at the cathode.[11,12] By co-depositing chitosan and nanocomponents, organic and inorganic hybrid hydrogels can be facilely obtained on the surface of the cathode, which has demonstrated important applications in electrical analysis, biosensor and protein assembly.[13,14] Herein, we co-deposit chitosan and a type of nanoplatelet, *i.e.* layered double hydroxides (LDHs), to generate a multilayered structure that mimics the natural brick-and-mortar structure.

School of Resource and Environmental Science and Hubei Biomass-Resource Chemistry and Environmental Biotechnology Key Laboratory, Wuhan University, Wuhan 430079, China. E-mail: shixwwhu@163.com; Tel: +86-27-68778501

† Electronic supplementary information (ESI) available. See DOI: 10.1039/c5tb01056j

LDHs are a class of octahedral ionic lamellar compounds, having a positively charged metal hydroxide layer and compensating anions. LDH has the general formula $[M_{1-x}^{2+}M_x^{3+}(OH)_2]^{x+}[A_{x/n}^{n-}]^{x-}\cdot mH_2O$ (where M^{2+} and M^{3+} are divalent and trivalent metals, respectively, and A^{n-} is the interlayer anion).[15] LDH nanoplatelets possess excellent anion exchange ability and a number of advantageous properties such as good biocompatibility, low cytotoxicity, uniform morphologies and sizes, chemical and thermal stabilities, large surface-to-volume ratio and strong adsorption ability.[16] These inherent properties enable LDHs to carry anionic biomolecules such as DNAs,[17] RNAs[18] and drugs.[18–20] In addition, there are studies about adsorption of proteins on the surface of LDH owing to its inherent positive charge.[21] However, most guest molecules are quickly released from LDHs due to the large edge to volume ratio of the LDHs.[22]

In this study, we co-electrodeposited chitosan and LDHs to generate a multilayered structure for stimuli sensitive protein release. The layered hybrid structure should provide a long pathway for the protein to diffuse out and thus reduce the burst release.[22] Insulin was selected as a model protein. Diabetic patients usually need exogenous insulin and an unpleasant daily injection.[23] It is necessary to develop on-demand insulin delivery systems that can release insulin according to the surrounding stimuli such as the presence of glucose,[24] electrical potentials,[25] pH changes,[26,27] light,[28] magnetic field,[29] temperature changes[30] and ultrasound.[31] We demonstrate that insulin release from the hybrid chitosan and INS-LDH hydrogel is responsive to pH, anions and electrical signals. Scheme 1 illustrates our experimental procedure. The hexagonal shaped LDHs were hydrothermally synthesized for insulin loading. The insulin loaded LDHs (INS-LDHs) were dispersed in a chitosan solution (pH 5) and co-deposited with chitosan hydrogel on a titanium plate by biasing a cathodic potential. EPD of the chitosan chains and INS-LDHs generated a hybrid hydrogel with multilayered structure, wherein the oriented LDHs were glued by chitosan. The release of insulin from the hydrogel was triggered by external stimuli, *i.e.* anions, pH changes or external potentials. This fast and simple EPD method to fabricate multilayered hybrid hydrogels and stimuli controlled drug release should expand the application of multilayered structures in drug-delivery systems.

2. Experimental

2.1. Materials

Chitosan with a deacetylation degree of 85% and a molecular weight of 200 kDa was purchased from Sigma and provided as a coarse powder. Insulin (bovine) was purchased from Sigma with a molecular weight of 5733.49 Da. Titanium plates with a thickness of 100 μm were purchased from Baoji Titanium Company, Shanxi. Magnesium chloride and aluminum chloride were purchased from Shanghai Reagent Co., Ltd (China). All reagents were of analytical grade and were used without further purification.

2.2. Preparation of layered double hydroxides

Layered double hydroxides, $Mg_2Al(OH)_6Cl\cdot xH_2O$ (Cl-LDHs), were prepared by a co-precipitation method in the presence of excess Mg^{2+} according to a previously reported approach with some modifications.[32] Briefly, $MgCl_2$ (2.28 g) and $AlCl_3$ (1.06 g) were dissolved in 80 ml water. The mixed salt solution was then added (within 5 s) to 320 ml NaOH solution (0.15 M) under vigorous stirring, followed by 15 min stirring, isolated from air. The precursor was collected by centrifugation (9000 rpm for 5 min) and washed twice. The precipitate was then dispersed in 140 ml deionized water and hydrothermally treated in an autoclave at 100 °C for 18 h. The LDH crystallites were obtained *via* centrifugation (16 000 rpm for 5 min) and washed twice, and then freeze-dried overnight for the following characterizations and protein loading. LDHs with anions of NO_3^- and CO_3^{2-} were also synthesized by a hydrothermal method (the detailed procedure is provided in the ESI†).

2.3. Insulin loading on layered double hydroxides

To load insulin on LDHs, 0.25 g of as-prepared LDHs was added to a 50 ml glycine–NaOH buffer solution (pH 8.6) containing 1.25 mg ml^{-1} insulin and stirred for 5 h at room temperature

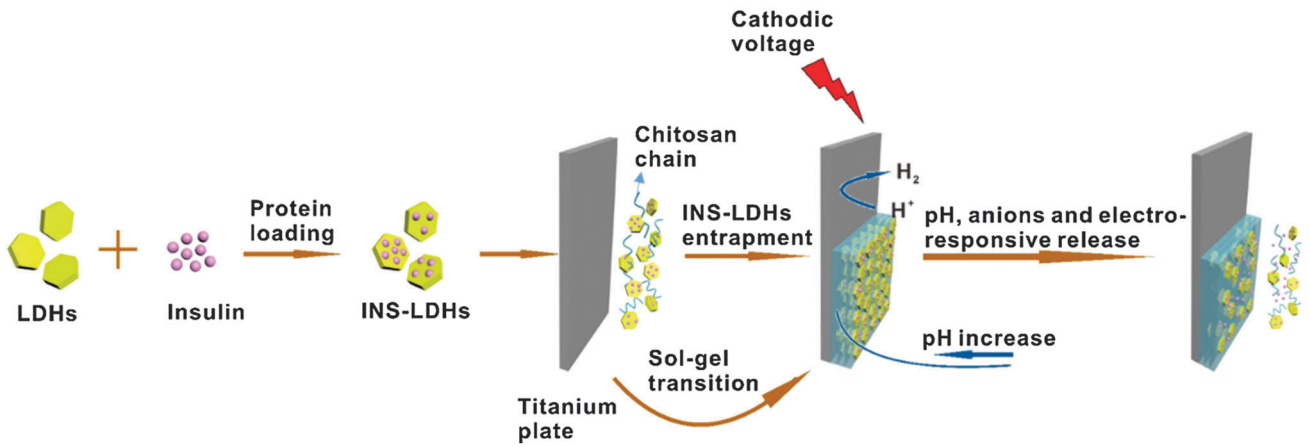

Scheme 1 Schematic of the procedure for the electrodeposition of multilayered chitosan/INS-LDHs hydrogel and stimuli-responsive insulin release.

until the adsorption reached equilibrium. Then, INS-LDHs were obtained by centrifugation (16 000 rpm for 5 min) and washed with glycine–NaOH buffer twice and freeze-dried overnight. The concentration of insulin in the supernatant was determined *via* UV absorption at 280 nm, followed by calibration using an insulin standard curve. The difference between the amount of insulin initially introduced and the protein content in the supernatant is taken as an indication of the amount of insulin entrapped.

The insulin loading capacity (LC) of INS-LDHs was defined as follows:

$$\mathrm{LC} = \frac{\mathrm{M1} - \mathrm{M2}}{\mathrm{M1} - \mathrm{M2} + \mathrm{M3}} \times 100\%$$

where M1 is the mass of insulin initially introduced, M2 is the mass of insulin in the supernatant, and M3 is the mass of LDHs initially introduced.

2.4. Electrodeposition of multilayered chitosan/INS-LDHs hydrogel

Briefly, a chitosan solution was prepared by dissolving chitosan flakes in a HCl solution (pH 3) under vigorous stirring and the undissolved flakes were removed by filtration. Before electrodeposition, the pH of the chitosan solution was adjusted to 5 by adding 1 mol l^{-1} NaOH, and NaCl was added to obtain a final concentration of 0.25% (w/v). A certain amount of INS-LDHs was then dispersed in 15 ml chitosan solution (1%, w/w) based on the mass ratio of chitosan to LDHs (3 : 1 to 1 : 2) and stirred for 30 min to obtain a homogeneous mixture. A titanium plate with a dimension of 4 cm × 2 cm × 100 μm was selected as the cathode for co-electrodeposition and cleaned with acetone, alcohol and water under sonication for 5 min each before deposition. The electrodeposition was carried out as follows: the titanium plate and a platinum wire were partially dipped into a chitosan solution (1%, w/v) and the distance between the two electrodes was maintained as 1 cm. A constant current (–0.75 mA cm^{-2}) was applied to the two electrodes for 30 min. The typical voltage for deposition was 3–4 V and the deposited hydrogel had a thickness of 2 mm. Then, the white hydrogel on the titanium plate was rinsed briefly with distilled water. The amount of INS-LDHs entrapped in the chitosan hydrogel was determined by dissolving the hydrogel in pH 1.2 HCl solution, followed by centrifugation. The concentration of insulin in the HCl solution was measured by its absorbance at 280 nm, as described above.

2.5. Anion responsive release of insulin from INS-LDHs and chitosan/INS-LDHs hydrogel

The release of insulin from INS-LDHs was performed in pH 9.0 solution containing 100 mM HPO_4^{2-}, SO_4^{2-}, CO_3^{2-}, Cl^- or NO_3^-. The release was also carried out in 1 mM, 5 mM or 10 mM phosphate buffer at pH 7.4. Typically, 0.15 g INS-LDHs was added to a 50 ml colorimetric tube, which contained the abovementioned solutions at 37 °C. At predetermined time intervals, 5 ml of the release medium was withdrawn and centrifuged at 16 000 rpm for 5 min. The insulin concentration in the supernatant was analyzed by UV-vis spectroscopy. Each assay was carried out in triplicate.

The release of insulin from the INS-LDHs hydrogel was carried out in a similar way. The electrodeposited hydrogel was immersed in 20 ml solution and the released insulin was measured by UV-vis. In some cases, the release buffer contained 0.1 M NO_3^-, Cl^-, or SO_4^{2-} and the pH of the solution was varied as 4.0, 7.0 or 9.0. Each assay was also carried out in triplicate.

2.6. Electrochemically controlled insulin release from chitosan/INS-LDHs hydrogel

A titanium plate with deposited chitosan/INS-LDHs hydrogel was partially immersed in 0.9% NaCl solution and a platinum wire was used as the counter electrode. The release of insulin was activated by applying a voltage of 0 V, 5 V or −5 V. In the case of 0 V, 0.9% NaCl solutions with different pHs (4.0, 7.0, and 9.0) were used as the release medium. In the on–off mode, the time sequence of the voltage was "on" for 30 min and "off" for 30 min, and the voltage was set as +5 V or −5 V. The release of insulin was monitored by the UV-vis method described above. Each assay was also carried out in triplicate.

2.7. Characterization of LDHs, INS-LDHs and chitosan/INS-LDHs

Transmission electron microscopy (TEM) was performed using a JEM-100CXII instrument. Field emission scanning electron microscopy (FE-SEM, ZEISS, Germany) was applied to observe the morphology of the LDHs and chitosan/INS-LDHs hydrogel. The size distribution and zeta potential of LDHs and INS-LDHs were determined by a Zetasizer 3690 (Malvern, UK) instrument. LDHs were dispersed in water and sonicated for 5 min before measurement. The distribution of ions at the surface of INS-LDHs was measured by an Energy Dispersive Spectrometer (EDS, XSAM800). X-ray diffraction (XRD) tests were carried out on an XRD diffractometer (D8-Advance, Bruker). The XRD patterns acquired with Cu K_α radiation (0.154 nm) at 40 kV and 40 mA were recorded in the 2θ range of 7°–80°. Samples for Fourier transform infrared (FT-IR) spectroscopy were vacuum dried overnight at 60 °C and recorded using the KBr pellet method on a Nicolet 5700 Fourier transform infrared spectrometer. The thermal behaviors of the samples were examined by thermogravimetric analysis (TGA, Shimadzu DTG-60) from room temperature to 600 °C at a heating rate of 5 °C min^{-1}. The absorbance at 280 nm for released insulin was measured by UV spectrophotometry (UV-1780, Shimadzu).

3. Results and discussion

Cl-LDHs were prepared by a co-precipitation method in the presence of excess Mg^{2+}.[32] The precursors (Mg–OH and Al–OH) for LDH synthesis were hydrothermally treated for 18 h at 100 °C. The SEM and TEM images of Cl-LDHs are shown in Fig. 1. Cl-LDHs have a well-defined hexagonal shape and the lateral size is in the range of 60–150 nm. From the TEM images, some single LDH plates can be found, which results in a larger

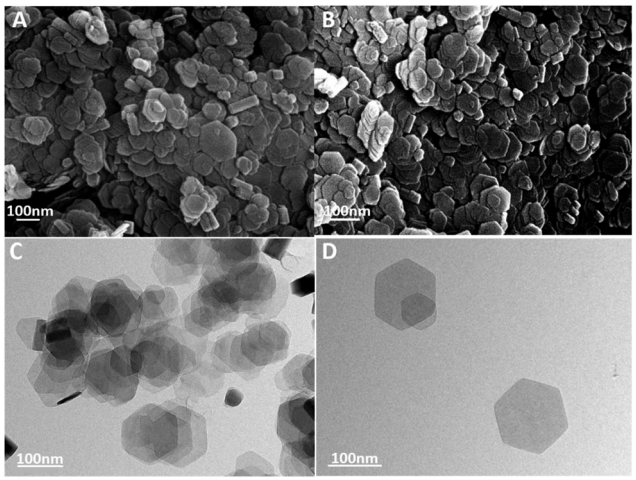

Fig. 1 SEM images (A) and (B), TEM images (C) and (D) of the Cl-LDHs.

surface area and facilitates further protein loading. The SEM images of LDHs with anions of NO_3^- and CO_3^{2-} (NO_3-LDHs and CO_3-LDHs) show aggregated sheets and particles (Fig. S1, ESI†). Furthermore, the insulin loading amount of CO_3-LDHs and NO_3-LDHs is lower than that of Cl-LDHs. Therefore, we used Cl-LDHs for insulin loading and hydrogel formation in the following experiments.

Insulin was then loaded on the LDH plates by incubating LDHs in glycine–NaOH buffer (pH 8.6) containing insulin for 5 h. The residue of insulin was removed by washing with glycine–NaOH buffer solution twice. The energy dispersive spectra (EDS) provide evidence of successful insulin loading on the LDHs (Fig. 2). There are mainly four elements (Mg, Al, O, and Cl) on the surface of the pristine LDHs (Fig. 2A). Elemental analysis indicates that the atomic ratio [Mg]/[Al] = 1.7–1.8 is slightly less than the designed value (2.0), which is due to leaching of more Mg^{2+} than Al^{3+} from the hydroxide layers.[33,34] After insulin loading (Fig. 2B), the appearance of the C, N and S peaks provides evidence that insulin was loaded on the surface of LDHs. The change of the size distribution of LDHs before and after insulin loading was measured by a Malvern laser particle size analyzer. The average hydrodynamic diameter of pristine LDHs dispersed in water is 68 nm, as shown in Fig. 2C, which is in accordance with the SEM and TEM analysis. The insulin loaded LDHs (Fig. 2D) show size distribution curves similar to that of the pristine LDHs, indicating that insulin loading did not change the diameter of LDHs.

However, the loading of insulin remarkably affected the surface charge of LDHs. LDHs had a zeta-potential of 8.62 mV at pH 7, which changed to −4.2 mV after the adsorption of insulin (Table 1). The insulin molecule (pI 5.3–5.4) contains negatively charged residues, for instance, aspartic acid and glutamic acid, showing a net charge of −19 mV at neutral pH. These residues would be attracted to the LDHs surface, resulting in INS-LDHs with negative charge because of charge compensation. This suggests that the insulin molecules exhibit electrostatic affinity for the LDHs surface and thus change the potential of the electrical double layer of the LDH nanoplatelets.[14,35,36]

The X-ray diffraction patterns of pristine LDHs and INS-LDHs are shown in Fig. 3A. LDHs exhibited a series of 00*l* Bragg reflections, which are the characteristic reflections of the LDHs layered structure. In the XRD pattern of INS-LDHs, the (003), (006) and (009) peaks did not show any noticeable shift. Furthermore, the basal spacing (d_{003}) of pristine LDHs is

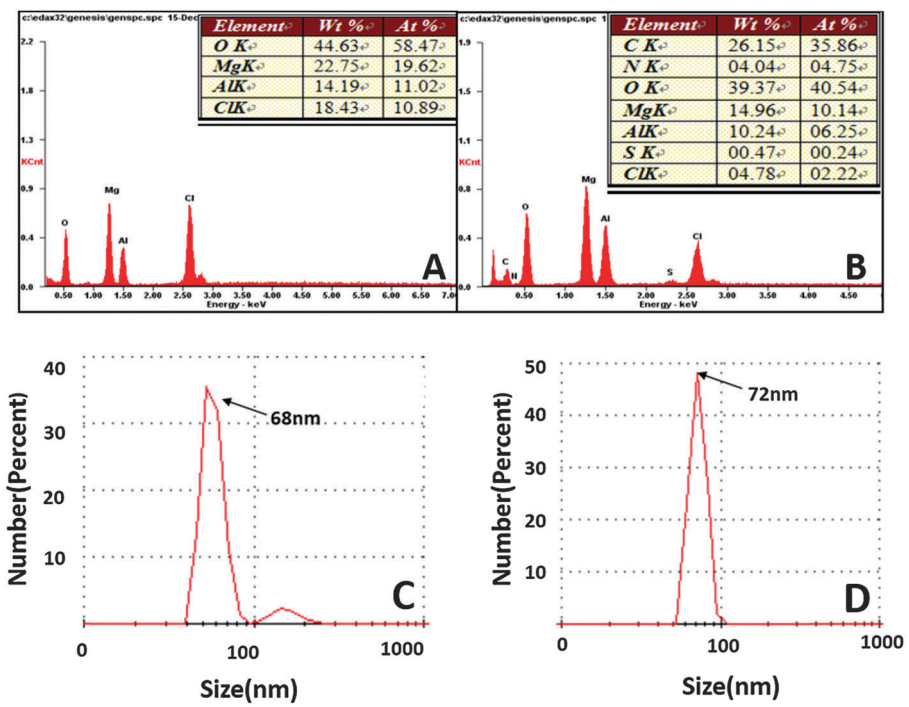

Fig. 2 EDS analysis of (A) LDHs, (B) INS-LDHs and the size distribution of (C) LDHs, (D) INS-LDHs.

Table 1 Zeta potentials of LDHs, insulin and INS-LDHs

Sample	LDHs	Insulin	INS-LDHs
Zeta potential (mV)	8.62	−19.43	−4.2

0.77 nm, which is identical with that of INS-LDHs.[37] Considering that the size of the insulin molecule is in the range of several nanometers, it is reasonable to conclude that no intercalation of LDHs by insulin occurred, and insulin was mainly adsorbed on the surface of LDHs.

Further evidence of insulin loading on LDHs was provided by FT-IR spectroscopy (Fig. 3B). In the FT-IR curve of pure insulin, absorption bands were detected at wavelengths of 1652 cm^{-1} and 1544 cm^{-1}. These bands were related to the functional groups found in insulin: amide I (protein C═O stretching) and amide II (protein N–H bend, C–N stretch).[38] In the spectrum of LDHs, the broad absorption band at around 3500 cm^{-1} was attributed to OH stretching due to the presence of hydroxyl groups on the LDHs. The absorbance at 1627 cm^{-1} was assigned to the bending vibrations of the interlayer water molecules.[33] Although the reactions were performed under a N_2 atmosphere, the strong absorbance at 1360 cm^{-1} indicated the existence of a small amount of CO_3^{2-}, which was due to unavoidable absorption of CO_2 by the basic solution.[39] In the FT-IR spectrum of INS-LDHs, the retention of the peaks at 1652 cm^{-1} and 1544 cm^{-1}, which are the characteristic peaks of insulin (amide I and amide II), and the peaks at 3500 cm^{-1} and 1360 cm^{-1} that originated from LDHs, provides further evidence that insulin was loaded on LDHs.

Fig. 3C displays the TG curves of insulin, LDHs and INS-LDHs. For insulin, the initial weight loss at 100 °C was caused by water evaporation, and the loss at 225 °C was associated with insulin decomposition. LDHs showed a weight loss starting at 60 °C owing to the loss of adsorbed and interlayer water. From 370 °C to 600 °C, the weight loss was mainly due to the dehydroxylation of the LDH sheets.[40] The onset of the degradation temperature (235 °C) for INS-LDHs is obviously lower than that of LDHs (370 °C), due to the presence of insulin in INS-LDHs. Because insulin is physically adsorbed on LDHs, the degradation temperature of INS-LDHs is close to that of insulin. The degree of weight loss during thermal analysis correlated closely with the amount of insulin loaded in the LDHs. Based on the weight loss ratios of insulin, LDHs and INS-LDHs, it can be estimated that the weight percentage of insulin in INS-LDHs is about 21%. By analyzing the difference between the amount of insulin initially introduced and the protein content in the supernatant, the insulin loading capacity (LC) was calculated to be 20.3%, which is comparable to that from TG analysis.

Since the electrostatic interaction plays an important role in insulin loading, the anions may have a profound effect on insulin release. We monitored the release of insulin by incubating INS-LDHs in pH 9 buffer containing 0.1 M HPO_4^{2-}, SO_4^{2-}, CO_3^{2-}, Cl^- or NO_3^-. From Fig. 4A, burst release of insulin was observed in buffers containing SO_4^{2-}, CO_3^{2-}, and HPO_4^{2-}, whereas relatively slow release was observed in the presence of Cl^- and NO_3^-. This phenomenon can be explained by the different binding competence between divalent and monovalent anions.[41] The release rate was also related to the concentration of anions. As shown in Fig. 4B, the release rate increased dramatically as the phosphate concentration increased, which is expected since at high concentration, phosphate ions have more opportunities to compete with Mg-sites and Al-sites.

The insulin release behavior can be adjusted by forming a multilayered structure with the chitosan hydrogel. Our previous study suggested that mesoporous silica nanoparticles can be co-deposited with the chitosan hydrogel.[11] When chitosan and LDHs were co-deposited, the electric field could align LDHs with the positive surfaces parallel to the electrode. This favorable parallel orientation was also observed for gibbsite nanoplatelet deposition under a direct-current electric field.[8] During the deposition, the localized sol–gel transition of chitosan and the electrophoretic deposition of nanoplatelets build the multilayered structure. The optical and SEM images of the deposited hydrogel (chitosan to LDHs ratio 1 : 1) are shown in Fig. 5. The pure chitosan hydrogel on the titanium plate was transparent (Fig. 5A) after deposition at −0.75 mA cm^{-2} for 30 min, whereas the co-deposition of chitosan and INS-LDHs resulted in an opaque hydrogel (Fig. 5D). The cross-section of the dried hydrogel was observed by scanning electron microscopy (SEM). Compared to the pure chitosan hydrogel (Fig. 5B and C), the chitosan/INS-LDHs hydrogel (Fig. 5E and F) revealed a multilayered structure. The enlarged image in Fig. 5F clearly

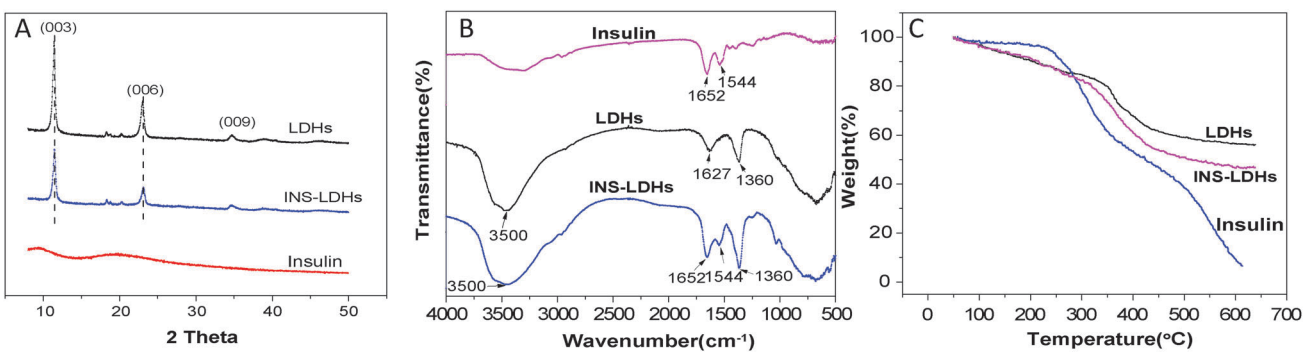

Fig. 3 X-ray diffraction pattern (A), FT-IR spectra (B) and TG curves (C) of LDHs, INS-LDHs and insulin.

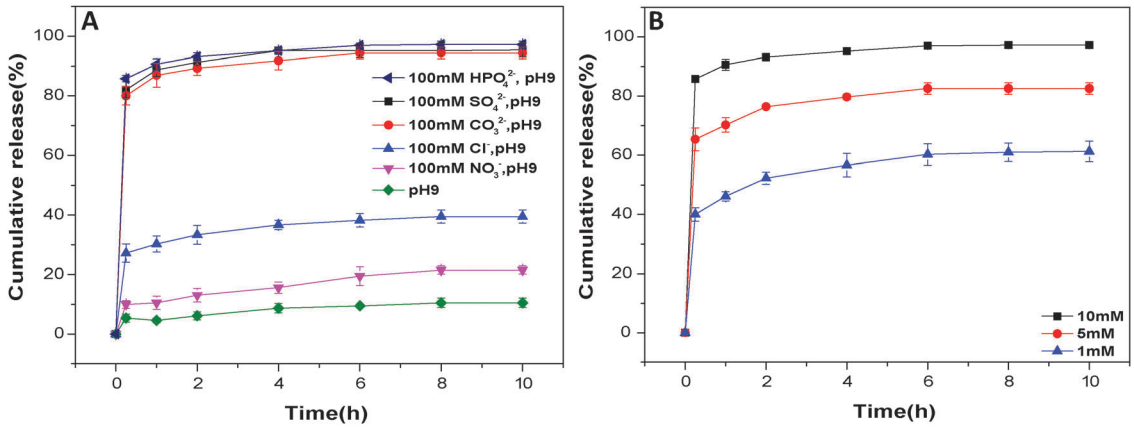

Fig. 4 Cumulative release profiles of insulin from (A) INS-LDHs in 100 mM HPO_4^{2-}, 100 mM SO_4^{2-}, 100 mM CO_3^{2-}, 100 mM Cl^- or 100 mM NO_3^- at pH 9 and (B) INS-LDHs in 10 mM, 5 mM or 1 mM phosphate buffer at pH 7.4.

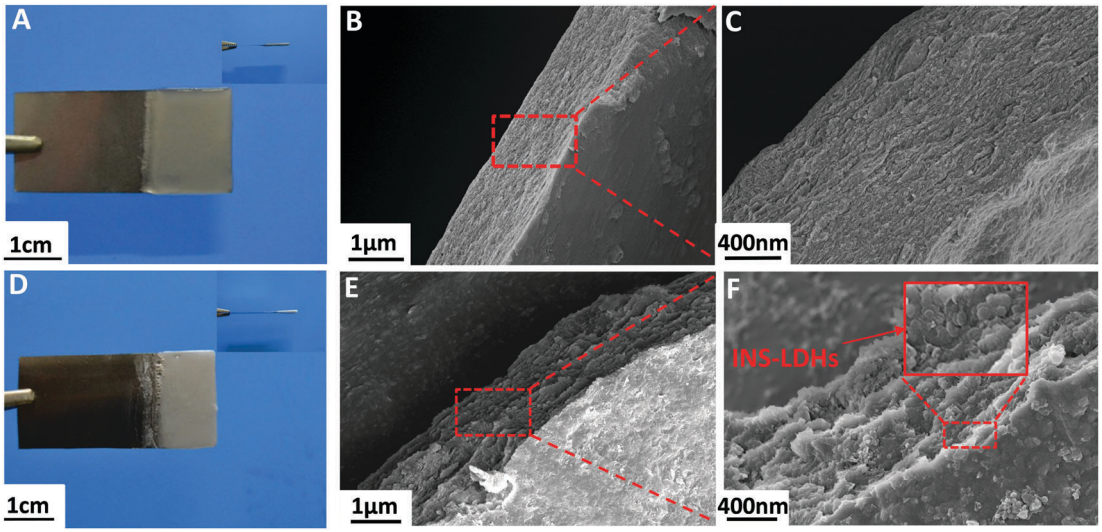

Fig. 5 Optical and SEM images of pure chitosan gel (A–C) and chitosan/INS-LDHs gel (chitosan to LDHs mass ratio 1 : 1) (D–F). The optical images show the hydrogel on titanium plate after deposition. The SEM images show the cross-section of the hydrogel.

showed the aligned LDHs in the chitosan hydrogel. Moreover, SEM images of the hydrogels with other chitosan to INS-LDHs ratios (3 : 1 to 1 : 2) are also provided in Fig. S2 (ESI†). The chitosan/LDHs films became more compact and less transparent with an increase in the ratio of the LDHs. In the case of a chitosan to LDHs ratio of 1 : 1, the amount of INS-LDHs deposited per cm^2 in the hydrogel could reach 2.5 mg cm^{-2}; however, for insulin this value was 0.5 mg cm^{-2}.

Formation of the multilayered chitosan/INS-LDHs hydrogel dramatically altered the release behavior of insulin. Firstly, the burst release of insulin, as demonstrated previously in Fig. 4A, was obviously reduced. The chitosan/INS-LDHs hydrogel was immersed in 0.1 M NO_3^- solution with different pH values (4.0, 7.0 and 9.0). At pH 9.0, the release of insulin from INS-LDHs reached 10% in the first 15 min and was only 4% after 2 h for chitosan/INS-LDHs (Fig. 6A), indicating that the multilayered structure retarded the protein release. Secondly, the release of insulin from chitosan/INS-LDHs was affected by the pH of the medium. The release at pH 4.0 and 9.0 was faster than that at pH 7.0. At pH 4.0, the electrostatic interactions between LDHs and insulin were reduced and the swelling of chitosan also facilitated the release of insulin. The different release behavior between pH 7.0 and 9.0 could be explained by the low solubility of insulin at neutral pH. Thirdly, the release can be adjusted by the presence of various anions. At pH 9.0, the release of insulin in 0.1 M NO_3^- was 10%, whereas sequentially changing the release medium to contain CO_3^{2-} and SO_4^{2-} did not reduce the release rate due to the different abilities of the anions to interact with Mg-sites and Al-sites. For comparison, the chitosan/INS-LDHs hydrogel was incubated in solutions of NO_3^- (0.1 M) only at different pH values for 8 h. It was observed that the release rate of insulin decreased gradually and reached equilibrium after 4 h (the release curves are plotted with dotted lines).

Inspired by the stimuli responsive release of insulin from the chitosan/INS-LDHs hybrid hydrogel, electrical signals were used to regulate the insulin release. The titanium plate with

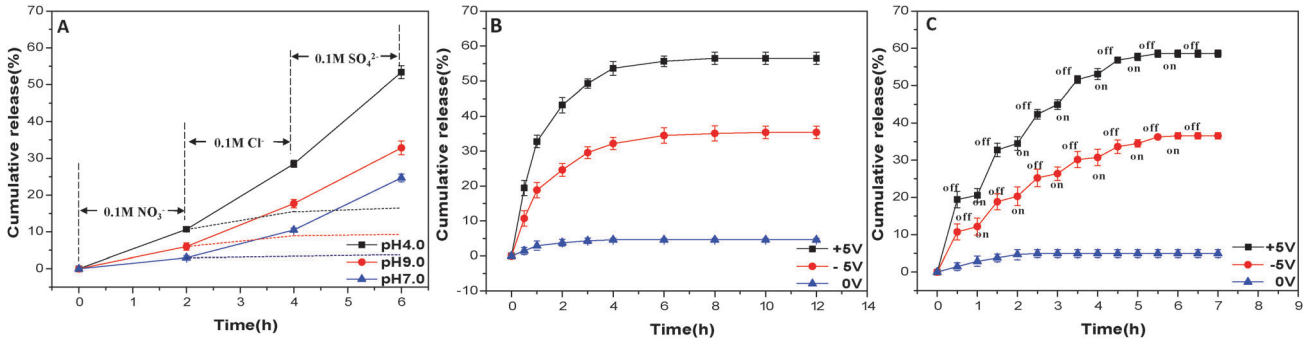

Fig. 6 Cumulative release profiles of insulin from chitosan/INS-LDHs. (A) The release was performed by sequentially changing anions under different pHs (the dotted lines show the continuous release in 0.1 M NO_3^-); (B) the insulin release by biasing different voltages; (C) step-wise release of insulin by adjusting the imposed on–off mode.

chitosan/INS-LDHs hydrogel was immersed in 0.9% NaCl solution and activated by applying a positive or negative potential. We first investigated the release behavior of insulin from the INS-LDHs hydrogel in 0.9% NaCl solution without applying a voltage but changing the pH as pH 4.0, pH 7.0 and pH 9.0. As indicated in Fig. S3 (ESI†), faster insulin release could be observed at pH 4.0 and pH 9.0. This observation is consistent with the results in Fig. 6A, in which slow release was found at neutral pH. However, the electrical stimulus tremendously accelerated the release of insulin when compared to the release under an unbiased potential (Fig. 6B). Over the course of 12 h, the cumulative release increased from 4.9% to 36.5% under application of −5.0 V and to 58.5% under +5.0 V. It was observed that the pH of the chitosan/LDHs hydrogel environment shifted under the potential. The pH of the hydrogel could increase from 7 to 8–9 under application of −5.0 V and decreased to 4–5 under application of +5.0 V. As discussed above, the change in the pH of the hydrogel environment induced by the applied potential adjusted the release behavior of insulin, leading to faster release than that at 0 V (pH 7.0). Therefore, electrical signals can be used to induce different release rates of insulin from the LDHs/chitosan hydrogel.

Finally, the release profile of insulin can be manipulated by switching the voltage in the on–off mode. The applied voltage was programmed as "on" for 30 min and then "off" for 30 min. A pulsed release pattern could be realized in response to the imposed electrical signals, although the step-wise release was more obvious in the first 4 h (Fig. 6C). It can be noted that positive potential (+5.0 V) had a more profound influence than negative potential (−5.0 V), which is in agreement with the results in Fig. 6B. When comparing the on–off release with the continuous release, the on-step contributed significantly to the release of insulin, while release in the off-step was quite slow. These results suggest that the release of insulin from the chitosan/INS-LDHs hydrogel could be tuned by applying different voltages.

4. Conclusions

By simultaneously electrodepositing chitosan and LDHs nanoplatelets, a multilayered chitosan/LDHs hybrid hydrogel was facilely fabricated, mimicking the brick-and-mortar structure in nature. The pH responsive and film forming property of chitosan and positively charged surface and the nanoscale dimensions of LDHs allow the gradual layer structure construction under an electric field. We explored the applicability of the nature inspired multilayered hydrogel as an insulin controlled release platform. External stimuli, such as pH, anion, and electrical potential, had a profound influence on the release of insulin. Notably, on-demand insulin release could be realized by programming the exerted electrical potentials. The present results suggest the advantage of electrodeposition in the construction of multilayered structures using stimuli-responsive natural polymers and nanocomponents as well as the great potential of the brick-and-mortar structure in controlled drug release.

Acknowledgements

This study was financially supported by the National Natural Science Foundation of China (Grant no. 51373124 and 21007049), the "Youth Chen-Guang Project" of Wuhan Bureau of Science and Technology (2014070404010196), the Program for New Century Excellent Talents in University (NECT-10-0618) and the Special Fund for Environmental Protection in the Public Interest (2013467064).

References

1 U. G. Wegst, H. Bai, E. Saiz, A. P. Tomsia and R. O. Ritchie, *Nat. Mater.*, 2015, **1**, 23–36.
2 L. J. Bonderer, A. R. Studart and L. J. Gauckler, *Science*, 2008, **319**, 1069–1073.
3 A. R. Studart, *Adv. Mater.*, 2012, **24**, 5024–5044.
4 S. Xia, Z. Wang, H. Chen, W. Fu, J. Wang, Z. Li and L. Jiang, *ACS Nano*, 2015, **9**, 2167–2172.
5 P. Y. Chen, A. Y. Lin, Y. S. Lin, Y. Seki, A. G. Stokes, J. Peyras, E. A. Olevsky, M. A. Meyers and J. Mckittrick, *J. Mech. Behav. Biomed. Mater.*, 2008, **1**, 208–226.
6 Y. Shu, P. Yin, J. Wang, B. Liang, H. Wang and L. Guo, *Ind. Eng. Chem. Res.*, 2014, **53**, 3820–3826.

7 W. Tong, X. Song and C. Gao, *Chem. Soc. Rev.*, 2012, **41**, 6103–6124.
8 T.-H. Lin, W.-H. Huang, I.-K. Jun and P. Jiang, *Chem. Mater.*, 2009, **21**, 2039–2044.
9 T.-H. Lin, W.-H. Huang, I.-K. Jun and P. Jiang, *Electrochem. Commun.*, 2009, **11**, 1635–1638.
10 K. Yan, F. Ding, W. E. Bentley, H. Deng, Y. Du, G. F. Payne and X.-W. Shi, *Soft Matter*, 2014, **10**, 465–469.
11 P. Zhao, H. Liu, H. Deng, L. Xiao, C. Qin, Y. Du and X. Shi, *Colloids Surf., B*, 2014, **123**, 657–663.
12 X. Shi, H. Wu, Y. Li, X. Wei and Y. Du, *J. Biomed. Mater. Res., Part A*, 2013, **101**, 1373–1378.
13 L.-Q. Wu, K. Lee, X. Wang, D. S. English, W. Losert and G. F. Payne, *Langmuir*, 2005, **21**, 3641–3646.
14 K. D. Patel, T.-H. Kim, E.-J. Lee, C.-M. Han, J.-Y. Lee, R. K. Singh and H.-W. Kim, *ACS Appl. Mater. Interfaces*, 2014, **6**, 20214–20224.
15 P. Benito, M. Herrero, F. Labajos and V. Rives, *Appl. Clay Sci.*, 2010, **48**, 218–227.
16 S. Y. Lee and J. H. Chang, *BMB Rep.*, 2011, **44**, 77–86.
17 S. Li, J. Li, C. J. Wang, Q. Wang, M. Z. Cader, J. Lu, D. G. Evans, X. Duan and D. O'Hare, *J. Mater. Chem. B*, 2013, **1**, 61–68.
18 L. Li, W. Gu, J. Chen, W. Chen and Z. P. Xu, *Biomaterials*, 2014, **35**, 3331–3339.
19 A. I. Khan, L. Lei, A. J. Norquist and D. O'Hare, *Chem. Commun.*, 2001, 2342–2343.
20 V. Ambrogi, G. Fardella, G. Grandolini and L. Perioli, *Int. J. Pharm.*, 2001, **220**, 23–32.
21 L. Jin, D. He, Z. Li and M. Wei, *Mater. Lett.*, 2012, **77**, 67–70.
22 J. HyeonáLee, *Chem. Commun.*, 2012, **48**, 5641–5643.
23 J. Liang, Y. Ma, S. Sims and L. Wu, *J. Mater. Chem. B*, 2015, **3**, 1281–1288.
24 A. Sinha, A. Chakraborty and N. R. Jana, *ACS Appl. Mater. Interfaces*, 2014, **6**, 22183–22191.
25 F. Ding, X. Shi, Z. Jiang, L. Liu, J. Cai, Z. Li, S. Chen and Y. Du, *J. Mater. Chem. B*, 2013, **1**, 1729–1737.
26 H. Sereshti, S. Samadi and M. Karimi, *RSC Adv.*, 2015, **5**, 9396–9404.
27 X. M. Li, Y. Y. Wang, J. M. Chen, Y. N. Wang, J. B. Ma and G. L. Wu, *ACS Appl. Mater. Interfaces*, 2014, **6**, 3640–3647.
28 N. C. Fan, F. Y. Cheng, J. a. A. Ho and C. S. Yeh, *Angew. Chem., Int. Ed.*, 2012, **51**, 8806–8810.
29 F. Liu and M. W. Urban, *Prog. Polym. Sci.*, 2010, **35**, 3–23.
30 S. W. Choi, Y. Zhang and Y. Xia, *Angew. Chem., Int. Ed.*, 2010, **49**, 7904–7908.
31 I. Tokarev and S. Minko, *Soft Matter*, 2009, **5**, 511–524.
32 Z. P. Xu, G. S. Stevenson, C.-Q. Lu, G. Q. Lu, P. F. Bartlett and P. P. Gray, *J. Am. Chem. Soc.*, 2006, **128**, 36–37.
33 Z. P. Xu and G. Q. Lu, *Chem. Mater.*, 2005, **17**, 1055–1062.
34 J. W. Boclair and P. S. Braterman, *Chem. Mater.*, 1999, **11**, 298–302.
35 K.-C. Yang, Z. Qi, C.-C. Wu, Y. Shirouza, F.-H. Lin, G. Yanai and S. Sumi, *Biochem. Biophys. Res. Commun.*, 2010, **393**, 818–823.
36 Y.-J. Shyong, R.-F. Lin, H.-S. Soung, H.-H. Wei, Y.-S. Hsueh, K.-C. Chang and F.-H. Lin, *J. Mater. Chem. B*, 2015, **3**, 2331–2340.
37 S. Li, J. Li, C. J. Wang, Q. Wang, M. Z. Cader, J. Lu, D. G. Evans, X. Duan and D. O'Hare, *J. Mater. Chem.*, 2012, **1**, 61–68.
38 H. P. Corporation, *Spectroscopy*, 2007, **21**, 151–160.
39 C. J. Wang and D. O'Hare, *J. Mater. Chem.*, 2012, **22**, 21125–21130.
40 Q. Z. Yang, D. J. Sun, C. G. Zhang, X. J. Wang and W. A. Zhao, *Langmuir*, 2003, **19**, 5570–5574.
41 T. Akazawa and M. Kobayashi, *J. Mater. Sci. Lett.*, 1996, **15**, 1319–1320.

